molecular pharmaceutics

Article

pubs.acs.org/molecularpharmaceutics

Development and Characterization of a Novel Mouse Line Humanized for the Intestinal Peptide Transporter *PEPT1*

Yongjun Hu,[†] Yehua Xie,[†] Yuqing Wang,[‡] Xiaomei Chen,[†] and David E. Smith*,[†]

[†]Department of Pharmaceutical Sciences, College of Pharmacy, University of Michigan, Ann Arbor, Michigan 48109, United States
[‡]College of Pharmaceutical Sciences, Zhejiang University, Hangzhou 310058, P. R. China

ABSTRACT: The proton-coupled oligopeptide transporter PEPT1 (SLC15A1) is abundantly expressed in the small intestine, but not colon, of mammals and found to mediate the uptake of di/tripeptides and peptide-like drugs from the intestinal lumen. However, species differences have been observed in both the expression (and localization) of PEPT1 and its substrate affinity. With this in mind, the objectives of this study were to develop a humanized *PEPT1* mouse model (*huPEPT1*) and to characterize hPEPT1 expression and functional activity in the intestines. Thus, after generating *huPEPT1* mice in animals previously nulled for mouse *Pept1*, phenotypic, PCR, and immunoblot analyses were performed, along with *in situ* single-pass intestinal perfusion and *in vivo* oral pharmacokinetic studies with a model dipeptide, glycylsarcosine (GlySar). Overall, the *huPEPT1* mice had normal survival rates, fertility, litter size, gender distribution, and body weight. There was no obvious behavioral or pathological phenotype. The mRNA and protein profiles indicated that *huPEPT1* mice had substantial PEPT1 expression in all regions of the small intestine (i.e., duodenum, jejunum, and ileum) along with low but measurable expression in both proximal and distal segments of the colon. In agreement with PEPT1 expression, the *in situ* permeability of GlySar in *huPEPT1* mice was similar to but lower than wildtype animals in small intestine, and greater than wildtype mice in colon. However, a species difference existed in the *in situ* transport kinetics of jejunal PEPT1, in which the maximal flux and Michaelis constant of GlySar were reduced 7-fold and 2- to 4-fold, respectively, in *huPEPT1* compared to wildtype mice. Still, the *in vivo* function of intestinal PEPT1 appeared fully restored (compared to *Pept1* knockout mice) as indicated by the nearly identical pharmacokinetics and plasma concentration−time profiles following a 5.0 nmol/g oral dose of GlySar to *huPEPT1* and wildtype mice. This study reports, for the first time, the development and characterization of mice humanized for *PEPT1*. This novel transgenic *huPEPT1* mouse model should prove useful in examining the role, relevance, and regulation of PEPT1 in diet and disease, and in the drug discovery process.

KEYWORDS: *PEPT1, humanized mice, mRNA and protein expression, glycylsarcosine, in situ intestinal perfusions, in vivo oral pharmacokinetics*

INTRODUCTION

Mammalian PEPT1 (SLC15A1), along with PEPT2 (SLC15A2), PHT1 (SLC15A4) and PHT2 (SLC15A3), belong to the solute carrier group of membrane transport proteins (i.e., SLC15) that mediate the cellular uptake of di- and tripeptides in addition to several peptidomimetic drugs. Following discovery of rabbit Pept1,[1] the human and mouse orthologues were cloned (85% amino acid identity)[2,3] in which they contained 708 and 709 amino acid residues, respectively. These Pept1 transporters have 12 transmembrane domains, C- and N-termini facing the cytoplasm, and Tyr12, His57, Tyr64, Trp294, Phe297, and Glu595 residues located within highly conserved transmembrane domains (H1, H2, H5, H7, and H10).[4]

In contrast to PEPT2, a high-affinity low-capacity transporter primarily responsible for the reabsorption of peptides/mimetics in kidney,[5] PEPT1 is a low-affinity high-capacity transporter that is important in the absorption of digested peptides (mostly di- and tripeptides) from dietary protein in the small intestine. PEPT1 is also crucial for the intestinal uptake and absorption of therapeutic drugs such as the β-lactam antibiotic cefadroxil[6] and the antiviral nucleoside prodrug valacyclovir.[7] Previous studies using polymerase chain reaction (PCR) and immunoblot analyses have demonstrated that in rodents and humans PEPT1 is abundantly expressed in the apical membrane of enterocytes in duodenal, jejunal, and ileal regions.[8−11] The expression of PEPT1 in colon is controversial and perhaps species dependent. Nevertheless, under normal conditions, PEPT1 is unlikely to have much impact on the absorption of peptides/mimetics from this region.

Species differences in PEPT1 expression and functional activity have been reported in mouse and human colonic tissue.[11,12] Moreover, our laboratory demonstrated *in vivo* that both cefadroxil[6] and valacyclovir[7] exhibited dose-proportional absorption in wildtype and *Pept1* knockout mice after oral dose escalation. The "apparent" dose linearity observed in these mouse studies is contrary to the nonlinear intestinal absorption kinetics reported in rats and humans for cefadroxil[13,14] and in humans for valacyclovir.[15] Interspecies differences in transporter-mediated activity are difficult to sort out given that

Received: July 22, 2014
Revised: August 15, 2014
Accepted: August 22, 2014
Published: August 22, 2014

   dx.doi.org/10.1021/mp500497p | *Mol. Pharmaceutics* 2014, 11, 3737−3746

Table 1. Primers Used in Quantitative Real Time PCR

gene[a]	forward primer (5′−3′)	reverse primer (5′−3′)
mGapdh (EC = 1.2.1.12)	GAGACAGCCGCATCTTCTTGT	CACACCGACCTTCACCATTTT
hPEPT1 (SLC15A1)	TGACCTCACAGACCACAACCA	GCCAGGCCGATCAAGGA
mPept1 (Slc15a1)	CCACGGCCATTTACCATACG	TGCGATCAGAGCTCCAAGAA
mPept2 (Slc15a2)	TGCAGAGGCACGGACTAGATAC	GGGTGTGATGAACGTAGAAATCAA
mPht1 (Slc15a4)	GCTGCCACCTGCATTACTACTTC	CGTACTTCACAGACACAATGAGGAA
mPht2 (Slc15a3)	GCTGAAGCTTGCGTTCCAA	AACAGGTGGGCACTTTCAGAGT
mBphl (EC = 3.1.-.-)	GCCAAGGTGGCTGTGAATG	GATCGCATGTTCCCCTTCTC
mAtb$^{0,+}$ (Slc6a14)	TCAGGATTTGACTTGGCATTCA	CAAGGCCCAATGTTAAAAGCA
mOat1 (Slc22a6)	CCACCTGCTAATGCCAACCT	GATTCGGGTCGTCCTTGCT
mOat2 (Slc22a7)	TGTCGCAAAGACCCTCGTACT	ACATCATCATGCAGCACAGTGA
mOat3 (Slc22a8)	GCCCCAGCCTCACTGTCTATAT	ACATTCAAGATAATGGTGCTCAGAGA
mOct1 (Slc22a1)	TGGTGTTCAGGCTGATGGAA	GCCCAAAACCCCAAACAAA
mMate1 (Slc47a1)	TTCTGCTTGTGACACGCTCAT	AGTGTCCCCCTTTGCAGGAT
mMate2 (Slc47a2)	GACATCATTTCCCTTGTGAGTCAA	GCCCGCAAGTGCATCAA
mPat1 (Slc36a1)	TCTGCTGTGTCTACTTCGTGTTTCT	GGATCACGGTCACATTGTTGTT

[a]Shown as gene name (solute carrier group or enzyme commission number) for human (h) and mouse (m) transporters or enzymes.

studies are usually performed by different investigators and laboratories and especially under varying experimental conditions. For this reason, we demonstrated in a single system, yeast *Pichia pastoris*, a species difference in the affinity of glycylsarcosine (GlySar) for rat, mouse, and human PEPT1 transformants.[16] These findings, and others, clearly illustrate that species differences may impact the intestinal absorption and pharmacokinetics of PEPT1 substrates, thereby, making it more difficult to predict systemic drug exposure. It is also clear that cell culture systems, naive or transfected with transporters of interest, as well as further *in vitro* or *in situ* methods, will not reflect what happens in humans under physiological conditions.

The past decade has shown a growing interest in the development of humanized mice to overcome species differences in drug metabolism, disposition, and regulation.[17−21] Studies with humanized mouse models not only provide a mechanistic understanding of species differences but also improve our ability to optimize and predict the pharmacokinetic, therapeutic, and safety profiles of xenobiotics in humans. With this in mind, the primary aim of this study was to generate a humanized *PEPT1* (*huPEPT1*) mouse model, which was nulled for the mouse *Pept1* gene and expresses the human transporter in the tissues where *Pept1* is normally expressed. The secondary aim was to characterize the *huPEPT1* mice with respect to hPEPT1 expression and functional activity in the intestines, as examined by *in situ* permeability and *in vivo* oral absorption studies with the model dipeptide GlySar.

EXPERIMENTAL SECTION

Chemicals. [^{3}H]-GlySar (98 mCi/mmol), [^{14}C]-GlySar (113 mCi/mmol), and [^{14}C]-inulin 5000 (1.1 mCi/g) were purchased from Moravek Biochemicals (Brea, CA). Unlabeled GlySar and inulin 5000 were purchased from Sigma-Aldrich (St. Louis, MO). Rabbit antihuman PEPT1 antiserum was generously provided by Dr. Hannelore Daniel (Technische Universität München, Germany). Protease inhibitor cocktail was purchased from Roche (Seattle, WA) and Power SYBR Green PCR Master Mix from Applied Biosystems (Foster City, CA). All other chemicals were obtained from standard sources.

Animals. Gender- and weight-matched mice (8 to 10 weeks) were provided in-house for *mPept1*$^{+/+}$ (wildtype), *mPept1*$^{-/-}$/*hPEPT1*$^{-/-}$ (*mPept1* knockout), and *mPept1*$^{-/-}$/*hPEPT1*$^{+/-}$ (humanized or *huPEPT1*) genotypes. All animals were bred on a C57BL/6 background (>99% congenic) in which the *Pept1* knockout and humanized mice were identified by genotyping and culled from the same litters. The mice were housed in a temperature-controlled environment with 12 h light and dark cycles and received a standard diet and water *ad libitum* (Unit for Laboratory Animal Medicine, University of Michigan, Ann Arbor, MI). All mouse studies were performed in accordance with the Guide for the Care and Use of Laboratory Animals as adopted and promulgated by the U.S. National Institutes of Health.

Generation and Molecular Characterization of Humanized *PEPT1* Mice. *huPEPT1* mice were generated using an approach described previously.[22] In brief, bacterial artificial chromosomes (BACs) containing the *PEPT1* gene were obtained from a human BAC library (Empire Genomics, Buffalo, NY). A BAC clone [RP11-782G13; ∼179 kb; CHR13 (98,091,462−98,270,723)], containing the entire 5′-terminal regulatory elements, coding area, and 3′-terminal regulatory elements, was then microinjected into the male pronucleus of fertilized one-cell embryos obtained from *Pept1*$^{-/-}$ mice on a C57BL/6 background.[23] The pronuclear stage embryos were then transferred into the uterus of pseudopregnant recipient animals. Founder mice were screened to identify an animal containing one copy of the human BAC after which these animals were bred (i.e., *mPept1*$^{-/-}$/*hPEPT1*$^{+/-}$ × *mPept1*$^{-/-}$/*hPEPT1*$^{-/-}$ mice) to maintain hemizygous transgenic lines.

Transgenic *huPEPT1* alleles were detected in offspring by PCR using genomic DNA isolated from tail biopsies. The first set had a forward primer 5′-ATCTTCTTCATCGTGGTCAATG-3′ and a reverse primer 5′-CCCAGCTGATGAAATTTGTGAA-3′, with a product size of 200 bp. The second set had a forward primer 5′-CCAATCTGCTCACACAGGATAGAGAGGGCAGG-3′ and a reverse primer 5′-CCTTGAGGCTGTCCAAGTGATTCAGGCCATCG-3′, with a product size of 524 bp. The endogenous *mPept1* gene was confirmed as nullified using a PCR approach described previously.[23] The PCR conditions were 1 cycle at 94 °C for 2 min, 35 cycles at 94 °C for 30 s, 53 °C for 45 s, and 72 °C for 60 s, and then 72 °C for 10 min.

Initial Phenotypic Analysis. The *huPEPT1* mice were evaluated for viability, fertility, serum clinical chemistry, and histology, as performed previously for wildtype and *Pept1* knockout mice.[23]

Real-time PCR and Immunoblot Analyses. Quantitation of *hPEPT1*, *mPept1*, *mPept2*, *mPht1*, *mPht2*, and other relevant genes was performed in the small intestine, colon, and kidney of wildtype, m*Pept1* knockout, and humanized *PEPT1* mice using a 7300 Real-Time PCR system (Applied Biosystems, Foster City, CA) as described before.[24] In brief, 2.0 μg of total RNA, isolated using the RNeasy Plus Mini Kit (Qiagen, Valencia, CA), was reversely transcribed into cDNA using the Omniscript RT Kit (Qiagen, Valencia, CA) with 16-mer random primers. The mouse *Gapdh* gene was used as an internal control of cDNA quality and quantity. The primers (Table 1) were designed using Primer 3.0 (Applied Biosystems, Foster City, CA) and synthesized by Integrated DNA Technologies (Coraville, IA). The real-time PCR thermal conditions were 1 cycle at 50 °C for 2 min, 1 cycle at 95 °C for 10 min, and then 40 cycles at 95 °C for 15 s and 60 °C for 1 min. The ΔCT method was used to calculate the relative levels of target gene transcripts in mice, where the ratio of target gene to *mGapdh* was equal to $2^{-\Delta CT}$, ΔCT = CT(*gene*) − CT (*mGapdh*).

Different segments of small intestine, colon, and kidney of wildtype, m*Pept1* knockout, and *huPEPT1* mice were homogenized in 2.0 mL of Nonidet P40-lysis buffer (50 mM Tris-HCl, 150 mM NaCl, 1% Nonidet P40, and proteinase inhibitor cocktail, pH 8.0), as described previously for immunoblot analyses.[12] The homogenates were sonicated for 10 pulses in ice at half strength, and then centrifuged at 15,000*g* at 4 °C for 15 min. The final concentration of proteins was measured with a BCA Protein Assay Kit (Pierce, Rockford, IL). The proteins were denatured at 40 °C for 45 min, resolved using 10% SDS-PAGE, transferred to a PVDF membrane (Millipore, Billerica, MA), and then blotted with specific rabbit antihuman PEPT1 antiserum[11] (1:3000 dilution) or specific rabbit antimouse PEPT1 antiserum[12] (1:5000 dilution).

***In Situ* Single-Pass Intestinal Perfusion Studies.** Wildtype, *mPept1* knockout, and humanized *PEPT1* mice were fasted overnight (∼12 h), but with free access to water, and anesthetized with sodium pentobarbital (40−60 mg/kg intraperitoneal). The permeability of GlySar in regional segments of the intestines (i.e., duodenum, jejunum, ileum, and colon) was then determined simultaneously, as described previously.[12] In brief, the mouse was placed on top of a heating pad to maintain body temperature, the abdominal area sterilized with 70% ethanol, and the intestine exposed by making an incision along its midline. A 4 cm segment of duodenum, 8 cm segment of proximal jejunum (∼2 cm distal to the ligament of Treitz), 6 cm segment of ileum (∼1 cm proximal to the cecum), and 4 cm segment of colon (∼0.5 cm distal to the cecum) was isolated and followed by incisions at both the proximal and distal ends. After the segment was rinsed with 0.9% isotonic saline solution, a glass cannula (2.0 mm outer diameter) was inserted at each end of the intestinal segment and secured in place with silk sutures. The isolated intestinal segment was covered with saline-wetted gauze and parafilm to prevent dehydration. After cannulation, the animals were then transferred to a temperature-controlled chamber at 31 °C to maintain body temperature during the entire perfusion procedure. The cannulas were then connected to inlet tubing that was attached to a 30 mL syringe (BD, Franklin Lakes, NJ USA) on a perfusion pump (Model 22: Harvard Apparatus, South Natick, MA) and to outlet tubing that was placed in a collection vial.

The perfusate buffer contained 135 mM NaCl, 5 mM KCl, and 10 mM MES/Tris (pH 6.5), plus 10 μM [^{3}H]-GlySar (0.5 μCi) and 0.01% (w/v) [^{14}C]-inulin-5000 (0.25 μCi), which severed as a nonabsorbable marker to correct for water flux during the perfusions. Buffer was perfused through each intestinal segment at a flow rate of 0.1 mL/min, and the exiting perfusate was collected every 10 min over a 90 min period. A 100 μL aliquot from each collection was added to a vial containing 6.0 mL of scintillation cocktail (Ecolite, MP Biochemicals, Solon, OH), and the samples were measured for radioactivity by a dual-channel liquid scintillation counter (Beckman LS 6000 SC, Beckman Coulter Inc., Fullerton, CA). At the end of experimentation, the length of all four intestinal segments was measured.

Concentration-dependent studies were also performed in the jejunum of wildtype and *huPEPT1* mice, by varying the perfusate concentrations of GlySar over a wide range (0.01−50 mM), to assess its saturable transport kinetics.

***In Vivo* Oral Pharmacokinetic Studies.** Following an overnight fast (∼12 h), wildtype, *mPept1* knockout, and *huPEPT1* mice were anesthetized briefly with isoflurane and administered 5.0 nmol/g [^{14}C]-GlySar (5.0 μCi/mouse in 0.2 mL normal saline) orally by gavage. After dosing, serial blood samples (15 μL) were collected at 5, 7.5, 15, 30, 45, 60, 90, 120, 180, 240, and 360 min via tail transections. The blood samples were placed in tubes containing 1.0 μL of EDTA-K3 and centrifuged at 3000*g* for 3 min to obtain plasma (∼5 μL). Animals were returned to their cages between blood sampling where they had free access to water and, 2 h after dosing, food. Radioactivity in the plasma samples was measured by a dual-channel liquid scintillation counter (Beckman LS 6000 SC, Beckman Coulter Inc., Fullerton, CA).

Data Analysis. The steady-state loss of drug from perfusate through the intestinal segments was achieved approximately 30 min after the start of perfusion. The effective permeability (P_{eff}) of drug was calculated according to a complete radial mixing parallel tube model:[25,26]

$$P_{eff} = \frac{-Q \ln(C_{out}/C_{in})}{2\pi RL}$$

where Q is the perfusion flow rate (0.1 mL/min), C_{out} is the outlet GlySar concentration after water flux correction, C_{in} is the inlet GlySar concentration, R is the internal radius (0.1 cm for small intestine and 0.2 cm for colon), and L is the length of intestinal segment.

The concentration-dependent flux (J) of GlySar in jejunum was best fit to a single Michaelis−Menten term in which[12]

$$J = P_{eff}C_{in} = \frac{V_m' C_{in}}{K_m' + C_{in}} = \frac{V_m C_w}{K_m + C_w}$$

where the parameters V_m' and K_m' were referenced to the inlet concentrations (C_{in}) and the parameters V_m and K_m were referenced to the intestinal wall concentrations (C_w) after correcting for the unstirred aqueous layer permeability.

Pharmacokinetic parameters, after oral dosing of GlySar, were determined using a noncompartmental approach (NCA, Phoenix WinNonlin v1.3, Certara, St. Louis, MO).

Data were reported as mean ± SE, unless otherwise noted. Statistical differences between two groups were determined by an unpaired t test. Multiple group comparisons were performed using one-way analysis of variance (ANOVA) followed by Dunnett's test in which wildtype mice served as the control

group (GraphPad Prism v5.0; GraphPad Software, Inc., La Jolla, CA). A value of $p < 0.05$ was considered significant.

RESULTS

Identification of *huPEPT1* Mice. Mice humanized for *PEPT1* were generated using a standard microinjection transgenic strategy with BAC DNA such that the entire *hPEPT1* genome, comprising all regulatory and coding regions, was integrated into the mouse chromosome for inheritance. As shown in Figure 1, PCR analysis of genomic DNA extracted from tail biopsies demonstrated that *hPEPT1* genomic DNA only appeared in *huPEPT1* ($mPept1^{-/-}/hPEPT1^{+/-}$) mice and the BAC clone RP11-782G13, which served as a positive control. In contrast, *hPEPT1* genomic DNA was not found in mouse genotypes $mPept1^{+/+}$ (wildtype), $mPept1^{-/-}/hPEPT1^{-/-}$ (*mPept1* knockout mice bred to hemizygous *huPEPT1* animals), and $mPept1^{-/-}$ (m*Pept1* knockout mice not bred to hemizygous *huPEPT1* animals). Using wildtype primers, mouse *Pept1* genomic DNA was neither detected in *huPEPT1* nor *Pept1* knockout mice (i.e., the $mPept1^{-/-}/huPEPT1^{-/-}$ and $mPept1^{-/-}$ genotypes). Since *mPept1* knockout primers were designed specifically to target the *Neo* gene, inserted during homologous recombination in the *Pept1* knockout mouse model,[23] a band was observed in $mPept1^{-/-}/hPEPT1^{+/-}$, $mPept1^{-/-}/huPEPT1^{-/-}$, and $mPept1^{-/-}$ mice, but not in $mPept1^{+/+}$ animals.

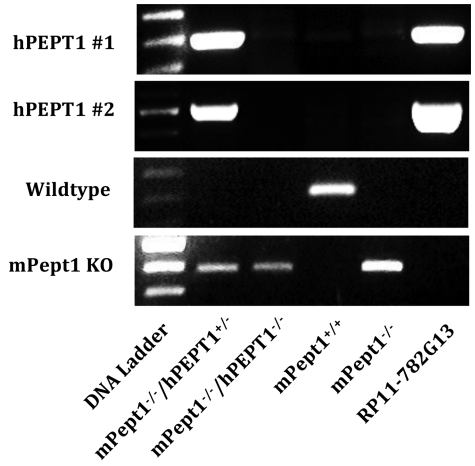

Figure 1. Genotyping results for the identification of humanized *PEPT1* mice. Genomic DNA was extracted from mouse tail biopsies and genotyped by PCR using specific primers, as described previously.[23] The DNA ladder, consisting of 100 bp repeats, was used to determine the size of PCR products. $mPept1^{-/-}/hPEPT1^{+/-}$ represents the positive screen for humanized *PEPT1* (*huPEPT1*) mice, $mPept1^{-/-}/hPEPT1^{-/-}$ the negative screen for humanized *PEPT1* mice, $mPept1^{+/+}$ the wildtype mice, $mPept1^{-/-}$ the *Pept1* knockout (KO) mice, and RP11−782G13 the purified BAC DNA (used to inject fertilized eggs in generating *huPEPT1*), which serves as a positive control.

During the process of generating *huPEPT1* mice, six founder mice were identified as containing the RP11-782G13 BAC DNA for *hPEPT1*. However, only five of these mice succeeded in germline transmission of the transgenic gene, and only three mouse lines showed *hPEPT1* transcripts (data not shown). The mouse line demonstrating the highest level of RNA was bred and maintained for subsequent studies. Using real-time PCR,[27] the integration copy number of BAC DNA transferred from the RP11-782G13 clone was estimated as one in our humanized *PEPT1* mouse genome.

Initial Phenotypic Analysis. Hemizygous *huPEPT1* mice appeared normal with no obvious behavioral abnormality as compared to wildtype and *mPept1* knockout ($mPept1^{-/-}$) mice. These humanized mice had normal survival rates, fertility, litter size, gender distribution, and body weight. Moreover, as shown in Table 2, there were no significant differences in serum clinical chemistry between the wildtype, *Pept1* knockout, and humanized *PEPT1* mice. Histologic evaluation (i.e., hematoxylin and eosin staining) established normal morphology of the kidney, small intestine, and cecum/colon across the three genetic strains (data not shown).

Table 2. Serum Clinical Chemistry of Wildtype (WT), Pept1 Knockout (KO), and Humanized PEPT1 (huPEPT1) Mice[a]

	WT	Pept1 KO	huPEPT1
Body Weight			
male, 7−8 weeks (g)	21.5 ± 0.6 (12)	21.3 ± 0.6 (12)	22.1 ± 0.5 (12)
female, 7−8 weeks (g)	17.9 ± 0.3 (12)	17.7 ± 0.4 (12)	18.0 ± 0.3 (12)
Serum			
sodium (mmol/L)	145 ± 1 (6)	147 ± 1 (6)	146 ± 1 (6)
potassium (mmol/L)	7.3 ± 0.5 (6)	7.4 ± 0.3 (6)	7.7 ± 0.5 (6)
chloride (mmol/L)	113 ± 1 (6)	113 ± 1 (6)	113 ± 1 (6)
calcium (mg/dL)	9.7 ± 0.5 (6)	9.5 ± 0.1 (6)	9.8 ± 0.2 (6)
albumin (g/dL)	3.4 ± 0.1 (6)	3.5 ± 0.1 (6)	3.6 ± 0.1 (6)
protein (g/dL)	6.4 ± 0.1 (6)	6.4 ± 0.1 (5)	6.3 ± 0.1 (4)
creatinine (mg/dL)	0.24 ± 0.03 (6)	0.25 ± 0.01 (6)	0.28 ± 0.05 (6)
bilirubin (mg/dL)	0.16 ± 0.05 (5)	0.08 ± 0.02 (5)	0.14 ± 0.02 (5)
glucose (mg/dL)	131 ± 22 (5)	163 ± 18 (6)	188 ± 6 (4)
BUN (mg/dL)	29.5 ± 2.4 (6)	27.5 ± 1.5 (6)	33.3 ± 2.1 (6)
ALT (U/L)	95.2 ± 16.0 (6)	78.0 ± 4.8 (6)	101 ± 6 (6)
ALP (U/L)	186 ± 29 (6)	94.2 ± 11.7 (6)	149 ± 15 (6)
AST (U/L)	124 ± 18 (6)	124 ± 16 (6)	104 ± 10 (6)

[a]Data are expressed as mean ± SE (n = number of mice). *Pept1* KO ($mPept1^{-/-}$) and *huPEPT1* ($mPept1^{-/-}/hPEPT1^{+/-}$) mice were not significantly different than WT ($mPept1^{+/+}$) mice, as evaluated by ANOVA/Dunnett's analyses. BUN is urea nitrogen, ALT is alanine aminotransferase, ALP is alkaline phosphatase, and AST is aspartate aminotransferase.

Stable Expression of hPEPT1 in the Intestine of Humanized Mice. Quantitative real-time PCR (qPCR) demonstrated that human (and not mouse) *PEPT1* transcripts were expressed in the small and large intestines of *huPEPT1* mice (Figure 2A), but not in wildtype and *Pept1* knockout animals (data not shown). Moreover, mouse *Pept1* transcripts were expressed in wildtype animals but these same transcripts were not observed in *Pept1* knockout mice (Figure 2A). A comparison of *Pept1* expression in proximal colon further demonstrated that *hPEPT1* mRNA was detectable in *huPEPT1* mice, whereas *mPept1* mRNA was not detectable in wildtype animals. Both *hPEPT1* and *mPept1* transcripts were observed in the distal colon, respectively, of *huPEPT1* and wildtype mice.

Immunoblot analyses of intestine and kidney were performed to assess whether the *hPEPT1* transcripts would be translated

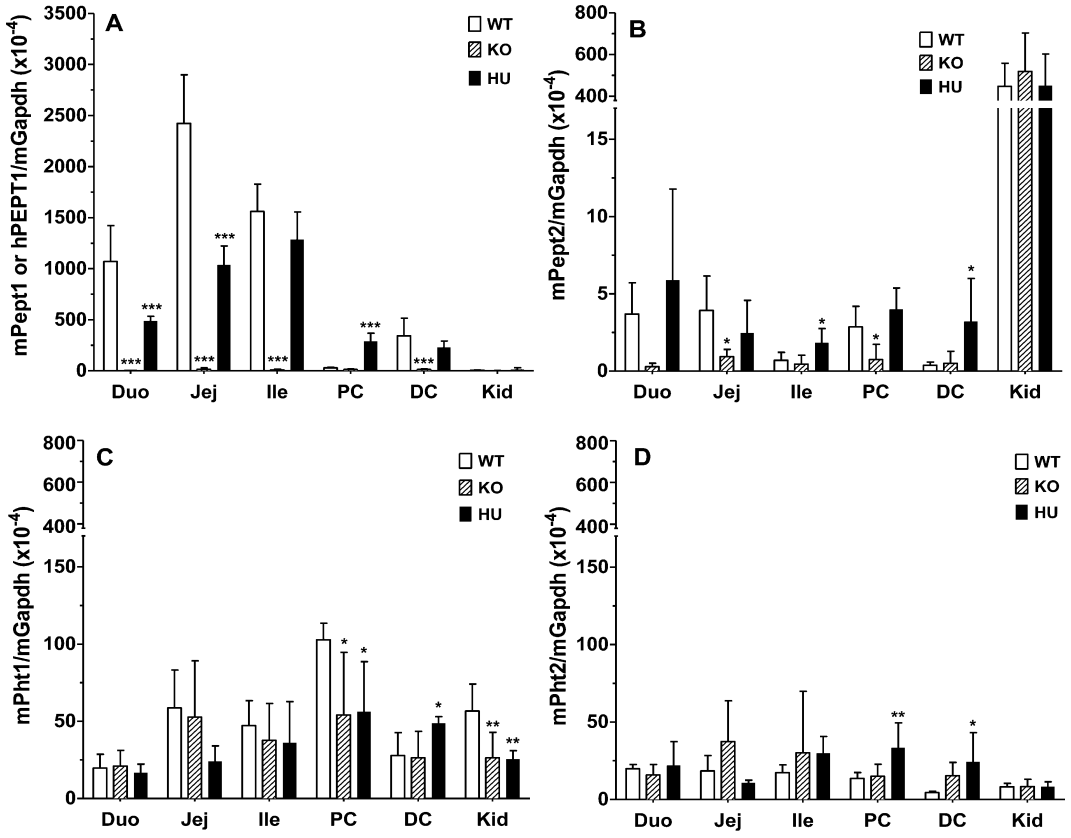

Figure 2. Real time-PCR analyses of *mPept1* or *hPEPT1* transcripts (A), *mPept2* transcripts (B), *mPht1* transcripts (C), and *mPht2* transcripts (D) in the small intestine, colon, and kidney of wildtype (WT = *mPept1*$^{+/+}$), *Pept1* knockout (KO = *mPept1*$^{-/-}$), and humanized *PEPT1* (HU = *mPept1*$^{-/-}$/*hPEPT1*$^{+/-}$) mice. Gene expression was normalized by *mGapdh*. Duo represents the duodenum, Jej the jejunum, Ile the ileum, PC the proximal colon, DC the distal colon, and Kid the kidney. Data are expressed as mean ± SE (n = 4–6). *p < 0.05, **p < 0.01, and ***p < 0.001, as evaluated by ANOVA/Dunnett's analyses in which WT was the control group. Note the discontinuous y-axis in panels B–D and the different scaling compared to panel A.

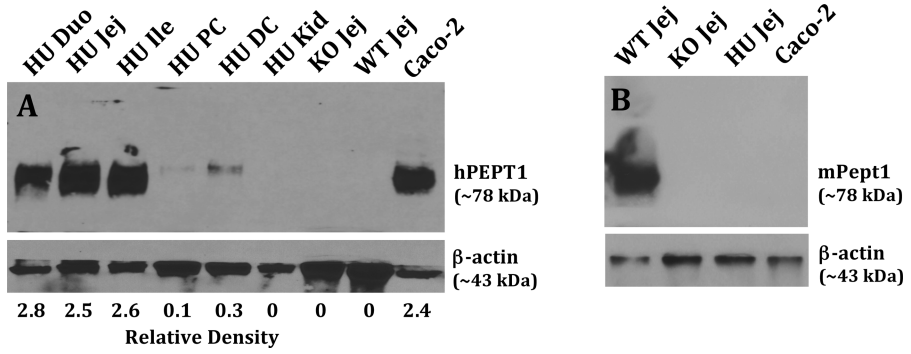

Figure 3. Immunoblots of hPEPT1 protein in the small intestine, large intestine, and kidney of wildtype (WT = *mPept1*$^{+/+}$), *Pept1* knockout (KO = *mPept1*$^{-/-}$), and humanized *PEPT1* (HU = *mPept1*$^{-/-}$/*hPEPT1*$^{+/-}$) mice (A), and mPEPT1 protein in the jejunum of the same genotypes (B). Protein samples were separated by 10% SDS-PAGE, transferred onto PVDF membranes, and incubated for 1.5 h with rabbit antihuman hPEPT1[11] (1:3000) or antimouse mPEPT1[12] (1:5000) antiserum, and a mouse monoclonal antibody for β-actin (1:1000). The membranes were washed three times with TBST and then incubated for 1 h with an appropriate secondary antibody of IgG conjugated to horseradish peroxidase (1:3000). Caco-2 cells served as positive and negative controls, respectively, for hPEPT1 and mPEPT1. Duo represents the duodenum, Jej the jejunum, Ile the ileum, PC the proximal colon, DC the distal colon, and Kid the kidney.

into protein. As observed in Figure 3A, high expression levels of hPEPT1 protein were noted in the duodenum, jejunum, and ileum of humanized *PEPT1* mice. In contrast, *huPEPT1* animals had low expression of PEPT1 protein in the proximal and distal colon, and no expression in kidney. Specificity of the rabbit antihuman PEPT1 antibody was confirmed by the absence of signal in jejunal samples from wildtype and *Pept1* knockout mice (Caco-2 cells served as a positive control). The presence of mPEPT1 protein was also tested in mice using a specific rabbit antimouse PEPT1 antibody, as shown in Figure 3B. In agreement with the qPCR results, mouse PEPT1 protein was expressed in the jejunum of wildtype mice, but not in the jejunum of *huPEPT1* and *mPept1* knockout animals (Caco-2 cells served as a negative control).

dx.doi.org/10.1021/mp500497p | *Mol. Pharmaceutics* 2014, 11, 3737–3746

Tissue Expression Profile of Select Transporters and Enzymes. It is crucial to know whether or not other proton-coupled oligopeptide transporters (POTs) will be dysregulated as a compensatory response to the mouse *Pept1* gene being replaced by a human *PEPT1* gene. As shown in Figure 2B–D, qPCR analyses indicated little to no expression of mouse *Pept2*, *Pht1*, and *Pht2* transcripts in the small and large intestines. There were moderate levels of *mPept2* mRNA in kidney; however, no change in expression was observed between the three genotypes (Figure 2B). In some cases, statistical differences were observed between the other three POT family members (Figures 2B–D). Nevertheless, given their extremely low expression levels, it is very unlikely that PEPT2 in the intestines and PHT1/2 in the intestines and kidney will have meaningful protein expression.

The tissue expression of several relevant peptide/mimetic transporters was also examined by qPCR. As shown in Figure 4, only minor changes were observed in mouse mRNA expression of transporters between the humanized *PEPT1* and *mPept1* knockout and wildtype animals. In this regard, m*Pat1* transcripts increased <2-fold in the small intestine of *huPEPT1* (compared to wildtype or knockout mice; Figure 4A), *mOat1* transcripts increased 2-fold in the kidney of *Pept1* knockout mice (although no difference was observed between wildtype and *huPEPT1* mice; Figure 4C), and *mOat2* transcripts increased 2-fold in the kidney of *huPEPT1* mice (compared to wildtype or knockout mice; Figure 4C). No differences were noted between the three genotypes in mouse mRNA expression of *mAtb*$^{0,+}$, *mOat3*, *mOct1*, *mMate1*, and *mMate2* in the small and large intestines and kidney.

The biphenyl hydrolase-like enzyme BPHL, important in activating the prodrug valacyclovir to acyclovir, was evaluated in the intestines and kidney by qPCR. A statistical decrease in mouse *Bphl* transcripts was observed in the small intestine of *Pept1* knockout mice (although no difference was observed between wildtype and *huPEPT1* mice; Figure 4A), and a statistical increase in mouse *Bphl* transcripts was observed in the large intestine of *huPEPT1* mice (compared to wildtype or knockout mice; Figure 4B). It is very unlikely, however, that BPHL will have meaningful protein expression in the intestines given their extremely low expression levels. Finally, no difference in mouse *Bphl* transcripts was observed between genotypes in the kidney (Figure 4C).

Primers used in the qPCR analyses can be found in Table 1.

***In Situ* Single-Pass Intestinal Perfusion Studies.** Intestinal perfusion studies were performed to evaluate the functional activity of PEPT1 in different regions of the small and large intestines, and to examine if differences exist between the three genotypes. As shown in Figure 5, there was substantial permeability of GlySar in the duodenum, jejunum, and ileum of *huPEPT1* mice, although the permeability was lower than that observed in wildtype animals. As expected, GlySar permeability was minimal, at best, in *Pept1* knockout mice in all intestinal regions. In agreement with the qPCR and immunoblot results, GlySar permeability was low, but measurable, in the colon of *huPEPT2* mice and about 11-fold higher than the colonic permeability observed in wildtype animals.

To assess if there were species-dependent differences in the transport kinetics of GlySar by PEPT1, concentration-dependent perfusion studies were performed in the jejunum of wildtype and *huPEPT1* mice. As shown in Figure 6A, the maximal flux (V_m' = 3.75 ± 0.11 nmol/cm^2/sec for wildtype and 0.50 ± 0.04 nmol/cm^2/sec for *huPEPT1*) and Michaelis

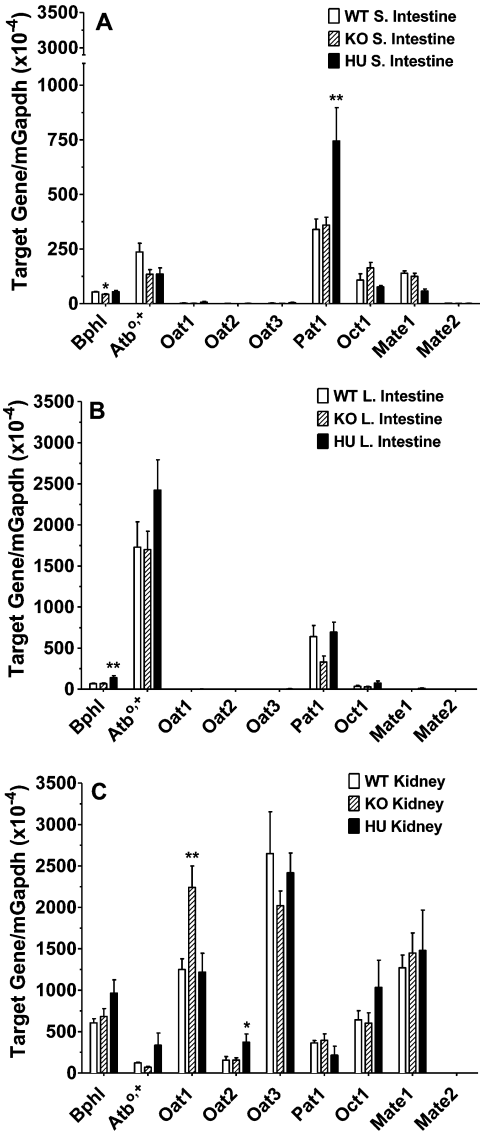

Figure 4. Real time-PCR analyses of select transporters and enzymes in the small intestine (A), large intestine (B), and kidney (C) of wildtype (WT = *mPept1*$^{+/+}$), *Pept1* knockout (KO = *mPept1*$^{-/-}$), and humanized *PEPT1* (HU = *mPept1*$^{-/-}$/*hPEPT1*$^{+/-}$) mice. Refer to Table 1 for gene identification. Data are expressed as mean ± SE (n = 4–6). *p < 0.05 and **p < 0.01, as evaluated by ANOVA/Dunnett's analyses in which WT was the control group. Note the discontinuous y-axis in panel A.

constant (K_m' = 13.2 ± 1.0 mM for wildtype and 3.3 ± 0.9 mM for *huPEPT1*) of GlySar were substantially lower in mice humanized for the *PEPT1* gene. When intestinal wall concentrations were used as the reference, after adjusting for the unstirred water layer, the maximal flux (V_m = 3.28 ± 0.13 nmol/cm^2/sec for wildtype and 0.49 ± 0.03 nmol/cm^2/sec for *huPEPT1*) and Michaelis constant (K_m = 5.5 ± 0.7 mM for wildtype and 2.7 ± 0.6 mM for *huPEPT1*) were similarly lower in *huPEPT1* mice as compared to wildtype animals (Figure 6B). These results demonstrate that a species difference exists in the transport kinetics of intestinal PEPT1.

***In Vivo* Oral Pharmacokinetic Studies.** To assess the *in vivo* functional activity of *hPEPT1* in humanized mice, the pharmacokinetics of the model dipeptide GlySar was evaluated after oral dosing. As shown in Figure 7, the plasma

dx.doi.org/10.1021/mp500497p | *Mol. Pharmaceutics* 2014, 11, 3737–3746

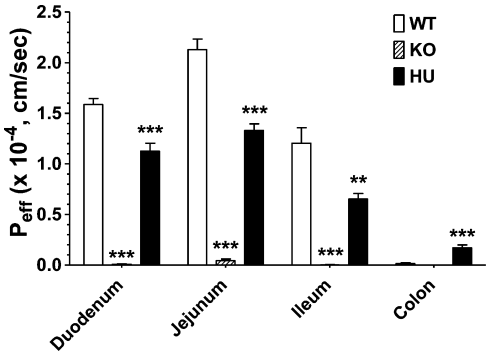

Figure 5. Effective permeability of 10 μM [^{3}H]-GlySar in different intestinal regions of wildtype (WT = *mPept1*$^{+/+}$), *Pept1* knockout (KO = *mPept1*$^{-/-}$), and humanized *PEPT1* (HU = *mPept1*$^{-/-}$/*hPEPT1*$^{+/-}$) mice. All studies were performed in pH 6.5 buffer. Data are expressed as mean ± SE (n = 4–6). $^{**}p < 0.01$ and $^{***}p < 0.001$, as evaluated by ANOVA/Dunnett's analyses in which WT was the control group.

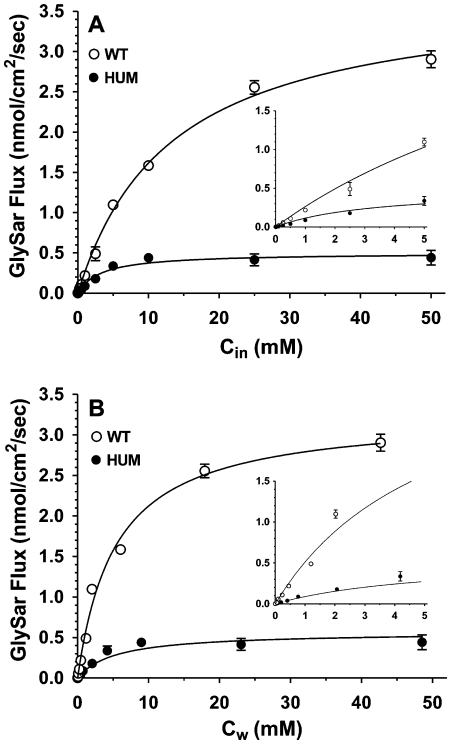

Figure 6. Concentration-dependent flux of [^{3}H]-GlySar (0.01–50 mM total substrate) during jejunal perfusions of wildtype (WT = *mPept1*$^{+/+}$) and *huPEPT1* (HU = *mPept1*$^{-/-}$/*hPEPT1*$^{+/-}$) mice. C_{in} is the inlet concentration of GlySar in perfusate in which V_m' = 3.75 ± 0.11 nmol/cm^2/sec and K_m' = 13.2 ± 1.0 mM for WT mice, r^2 = 0.988; V_m' = 0.50 ± 0.04 nmol/cm^2/sec and K_m' = 3.3 ± 0.9 mM for HU mice, r^2 = 0.838 (A). C_w is the estimated concentration of GlySar at the membrane wall in which V_m = 3.24 ± 0.13 nmol/cm^2/sec and K_m = 5.5 ± 0.7 mM for WT mice, r^2 = 0.993; V_m = 0.49 ± 0.03 nmol/cm^2/sec and K_m = 2.7 ± 0.6 mM for HU mice, r^2 = 0.973 (B). All studies were performed in pH 6.5 buffer. Data are expressed as mean ± SE (n = 4–6).

concentrations of GlySar were substantially reduced in *Pept1* knockout mice, and according to Table 3, all pharmacokinetic parameters were significantly different than wildtype animals. The systemic exposure (AUC) of GlySar in *Pept1* knockout mice was about 50% of that observed in wildtype animals. In contrast, the plasma concentration–time profiles of GlySar in

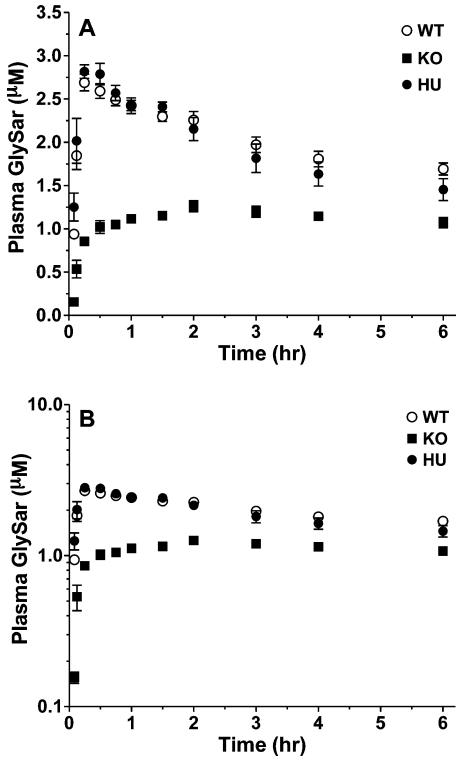

Figure 7. Plasma concentration–time profiles of [^{14}C]-GlySar in wildtype (WT = *mPept1*$^{+/+}$), *Pept1* knockout (KO = *mPept1*$^{-/-}$), and humanized *PEPT1* (HU = *mPept1*$^{-/-}$/*hPEPT1*$^{+/-}$) mice following a 5.0 nmol/g oral dose. Data are expressed as mean ± SE (n = 3) in which the y-axis is displayed on a linear scale (A) and on a logarithmic scale (B).

Table 3. Noncompartmental Pharmacokinetics of [^{14}C]GlySar after a 5.0 nmol/g Oral Dose in Wildtype (WT), Pept1 Knockout (KO), and Humanized PEPT1 (huPEPT1) Mice[a]

parameter (units)	WT	Pept1 KO	huPEPT1
C_{max} (μM)	2.71 ± 0.09	1.27 ± 0.05[b]	2.86 ± 0.09
T_{max} (h)	0.33 ± 0.08	1.83 ± 0.17[b]	0.33 ± 0.08
$AUC_{0-0.5}$ (μM·h)	1.12 ± 0.02	0.34 ± 0.01[b]	1.04 ± 0.04
AUC_{0-2} (μM·h)	4.76 ± 0.12	2.04 ± 0.04[b]	4.61 ± 0.04
AUC_{0-6} (μM·h)	11.6 ± 0.6	6.66 ± 0.25[b]	12.1 ± 0.3

[a]Data are expressed as mean ± SE (n = 3). [b]$^{***}P < 0.001$, as evaluated by ANOVA/Dunnett's analyses of WT (*mPept1*$^{+/+}$), *Pept1* KO (*mPept1*$^{-/-}$), and *huPEPT1* (*mPept1*$^{-/-}$/*hPEPT1*$^{+/-}$) mice, where WT was the control group.

huPEPT1 mice were virtually superimposable with that observed in wildtype animals. Humanized *PEPT1* and wildtype mice had the same values for C_{max} and T_{max}, suggesting that the absorption rate was not different between the two genotypes. Moreover, the incremental AUC values (i.e., AUC_{0-t}) in *huPEPT1* mice were 93%, 97%, and 104% of that in wildtype mice at 0.5, 2, and 6 h, respectively, indicating that PEPT1 activity had been fully restored in these mice.

DISCUSSION

Substantial progress has been made in generating and characterizing mice that contain human CYP450 and conjugation enzymes[19,20] and nuclear receptors.[20,21] However, with the exception of studies by Schinkel and co-workers[28–30]

dx.doi.org/10.1021/mp500497p | *Mol. Pharmaceutics* 2014, 11, 3737–3746

in which several organic anion-transporting polypeptide (OATP) transporters were humanized in mice and Scheer et al.[31] in which mice were humanized for multidrug resistance-associated protein 2 (MRP2), no other plasma membrane transporters have been humanized to date. Thus, the ability to generate a *huPEPT1* mouse model containing the entire human genome offers an unparalleled opportunity to more reliably study *in vivo* systems in human PEPT1 absorption, transport, pharmacologic response, disease, and regulation.

In the present study, we developed and characterized a novel mouse line humanized for *PEPT1*. In doing so, we made the following observations: (1) *huPEPT1* mice had no obvious behavioral or pathological phenotype; (2) mRNA and protein profiles indicated that *huPEPT1* mice had substantial PEPT1 expression in all regions of the small intestine (i.e., duodenum, jejunum, and ileum) along with low but measurable expression in both proximal and distal segments of the colon; (3) the *in situ* permeability of GlySar in *huPEPT1* mice was similar to but lower than wildtype animals in small intestine, and greater than wildtype mice in colon; (4) a species difference existed in the *in situ* transport kinetics of jejunal PEPT1, in which the maximal flux and Michaelis constant of GlySar were reduced in *huPEPT1* compared to wildtype mice; and (5) the *in vivo* function of intestinal PEPT1 appeared fully restored (compared to *Pept1* knockout mice) as indicated by the nearly identical pharmacokinetics and plasma concentration−time profiles of GlySar in *huPEPT1* and wildtype mice following a single oral dose.

There is good agreement among species (e.g., rat, mouse, and human) regarding the abundant protein expression of PEPT1 in duodenal, jejunal, and ileal segments of small intestine, and its apical localization.[8−12,32−35] However, the colonic expression of PEPT1 is controversial and may be the result of differences among species, antibody specificity, regional specificity, and the methods of preparation between different laboratories. Whereas some studies have reported the expression of PEPT1 protein in normal mouse, rat, and human colon,[9,11,32] other studies have been unable to detect PEPT1 in normal colon.[8,12,33−35] In particular, Wuensch et al.[11] found a distinct spatial distribution of colonic PEPT1 in mice, rats, and humans in which immunostaining was not observed in proximal colon, but significant staining was observed in the distal colon. In our hands, we have consistently detected abundant expression of PEPT1 protein in all regions of mouse and rat small intestine, but not in the colon of rodents past 7 days of age.[8,12] In addition, the functional activity of mouse PEPT1 was consistent with these expression levels, as determined by the permeability of GlySar,[12] cefadroxil,[36] and valacyclovir[37] in wildtype compared to *Pept1* knockout mice. In the present study, *huPEPT1* mice had measurable expression of PEPT1 protein in the distal and proximal colon (distal > proximal) and 11-fold higher permeabilities of GlySar in colon as compared to wildtype mice. Still, the colonic permeability of GlySar was only about 25−30% of that in ileum. Therefore, it appears that *huPEPT1* mice (under regulatory control of the human genome) could express a functional PEPT1 protein that transported GlySar across the colon, whereas wildtype mice (under regulatory control of the murine genome) did not have this capability.

A species-dependent difference was also reported in the affinity of PEPT1 for GlySar where the K_m values varied over a 5.4-fold range in yeast *Pichia pastoris* expressing the human (0.86 mM), mouse (0.30 mM), and rat (0.16 mM) transformants.[16] In the present study, this trend was reversed in which the K_m of GlySar was 2- to 4-fold lower (i.e., greater affinity), and the V_m or V_m' was 7-fold lower in *huPEPT1* mice compared to wildtype animals during *in situ* jejunal perfusions of substrate. It is unclear, at present, why the K_m values of GlySar "flip-flop" when studied *in vitro* in yeast expressing PEPT1 mouse and human homologues compared to *in situ* during intestinal perfusions in wildtype and *huPEPT1* mice. Thus, it will be important to determine, in subsequent studies, if the *in vivo* intestinal absorption of GlySar (and other peptides/mimetics) is dose-dependent (nonlinear) following oral dose escalation. In doing so, the *huPEPT1* mouse model might be useful in clarifying the discrepancy between the dose-proportional absorption of cefadroxil[6] and valacyclovir[7] in mice over an 8- to 10-fold oral dose range, respectively, and the nonlinear intestinal absorption observed for these compounds in humans.[14,15] More important, perhaps, would be the ability of *huPEPT1* mice to better predict the oral drug (and prodrug) performance of new chemical entities.

Previous studies have shown that, after oral dosing, the *in vivo* systemic exposure of GlySar in *Pept1* knockout mice was only about 50% of that in wildtype mice even though *in situ* permeabilities in the proximal small intestine differed by >10-fold between genotypes.[12,39] To explain this "apparent" discrepancy, the authors suggested that GlySar may be able to take advantage of the intestine's residual length and long residence times so that passive absorption processes play a bigger role in the absence of PEPT1. Our current study corroborated these earlier findings where GlySar had a substantially reduced (>50-fold) *in situ* permeability in the small intestine of *Pept1* knockout mice but an *in vivo* oral availability that differed by only 50%, compared to wildtype animals. Given the complexity of intestinal absorption (including membrane permeability, luminal drug concentration, and gastrointestinal residence time), it was not surprising that the pharmacokinetics and oral absorption profiles of GlySar were similar in wildtype and *huPEPT1* mice (Figure 7 and Table 3), especially when *in situ* permeabilities in the small intestine of *huPEPT1* mice were reduced by only 30−40% and higher in colon (Figure 5). However, since species differences were observed in the transport kinetics (i.e., V_m and K_m) of GlySar, it will be interesting to see whether or not the pharmacokinetics are similar in wildtype and *huPEPT1* mice when higher oral doses of substrate are administered and the chance of intestinal PEPT1 saturability increases.

It should be appreciated that transgenic mice were generated previously[38] in which *hPepT1* expression was regulated by the mouse β-actin or villin promoters as a model for studying the role of PEPT1 in inflammatory bowel disease. However, in these mice there was no deletion of endogenous mPEPT1. As a result, the concomitant protein expression of mouse and human PEPT1 in the intestines and other PEPT1-expressing tissues of the body make it impossible to separate the role of each species-specific transporter and, thereby, humanize the mouse. In our *huPEPT1* mouse model, the purified BAC DNA, containing the entire *hPEPT1* genome, was injected into eggs from *Pept1* knockout mice. As a result, the *huPEPT1* mice lacked endogenous mPEPT1 protein and, by maintaining the mice as hemizygotes, were able to avoid the potential interference of other endogenous genes. Another advantage of using genomic DNA was that transcripts of the *huPEPT1* gene were regulated by their own regulatory elements and

produced PEPT1 protein only if the gene translation mechanism was conserved among mammals.

In concluding, the present study reports, for the first time, the development and initial characterization of *huPEPT1* mice. These mice are unique in that they contain a copy of the entire human genome in mice previously nulled for *mPept1* and demonstrate the full restoration of PEPT1 function. There is excellent agreement between hPEPT1 expression in the intestines, the *in situ* intestinal permeability of GlySar, and the *in vivo* intestinal absorption of GlySar following a single oral dose. However, a clear species difference was observed in the maximal flux and affinity of GlySar during *in situ* jejunal perfusions of *huPEPT1* mice as compared to wildtype animals. These humanized *PEPT1* mice should prove a valuable model in future studies investigating the role, relevance, and regulation of PEPT1 in diet and disease and in the drug discovery process.

AUTHOR INFORMATION

Corresponding Author

*(D.E.S.) Tel: 734-647-1431 Fax: 734-763-3438. E-mail: smithb@umich.edu.

Notes

The authors declare no competing financial interest.

ACKNOWLEDGMENTS

We greatly appreciate the expertise of the Transgenic Animal Model Core, University of Michigan, in helping us to generate the *huPEPT1* mice. This work was supported by Public Health Service grant GM-035498 from the National Institute of General Medical Sciences (to D.E.S.).

REFERENCES

(1) Fei, Y. J.; Kanai, Y.; Nussberger, S.; Ganapathy, V.; Leibach, F. H.; Romero, M. F.; Singh, S. K.; Boron, W. F.; Hediger, M. A. Expression cloning of a mammalian proton-coupled oligopeptide transporter. *Nature* **1994**, *368*, 563−566.

(2) Liang, R.; Fei, Y. J.; Prasad, P. D.; Ramamoorthy, S.; Han, H.; Yang-Feng, T. L.; Hediger, M. A.; Ganapathy, V.; Leibach, F. H. Human intestinal H+/peptide cotransporter. Cloning, functional expression, and chromosomal localization. *J. Biol. Chem.* **1995**, *270*, 6456−6463.

(3) Fei, Y. J.; Sugawara, M.; Liu, J. C.; Li, H. W.; Ganapathy, V.; Ganapathy, M. E.; Leibach, F. H. cDNA structure, genomic organization, and promoter analysis of the mouse intestinal peptide transporter PEPT1. *Biochim. Biophys. Acta* **2000**, *1492*, 145−154.

(4) Smith, D. E.; Clemencon, B.; Hediger, M. A. Proton-coupled oligopeptide transporter family SLC15: physiological, pharmacological and pathological implications. *Mol. Aspects Med.* **2013**, *34*, 323−336.

(5) Ocheltree, S. M.; Shen, H.; Hu, Y.; Keep, R. F.; Smith, D. E. Role and relevance of peptide transporter 2 (PEPT2) in the kidney and choroid plexus: in vivo studies with glycylsarcosine in wild-type and PEPT2 knockout mice. *J. Pharmacol. Exp. Ther.* **2005**, *315*, 240−247.

(6) Posada, M. M.; Smith, D. E. In vivo absorption and disposition of cefadroxil after escalating oral doses in wild-type and PepT1 knockout mice. *Pharm. Res.* **2013**, *30*, 2931−2939.

(7) Yang, B.; Hu, Y.; Smith, D. E. Impact of peptide transporter 1 on the intestinal absorption and pharmacokinetics of valacyclovir after oral dose escalation in wild-type and PepT1 knockout mice. *Drug Metab. Dispos.* **2013**, *41*, 1867−1874.

(8) Shen, H.; Smith, D. E.; Brosius, F. C., 3rd. Developmental expression of PEPT1 and PEPT2 in rat small intestine, colon, and kidney. *Pediatr. Res.* **2001**, *49*, 789−795.

(9) Ziegler, T. R.; Fernandez-Estivariz, C.; Gu, L. H.; Bazargan, N.; Umeakunne, K.; Wallace, T. M.; Diaz, E. E.; Rosado, K. E.; Pascal, R. R.; Galloway, J. R.; Wilcox, J. N.; Leader, L. M. Distribution of the H+/peptide transporter PepT1 in human intestine: up-regulated expression in the colonic mucosa of patients with short-bowel syndrome. *Am. J. Clin. Nutr.* **2002**, *75*, 922−930.

(10) Walker, D.; Thwaites, D. T.; Simmons, N. L.; Gilbert, H. J.; Hirst, B. H. Substrate upregulation of the human small intestinal peptide transporter, hPepT1. *J. Physiol.* **1998**, *507* (Pt 3), 697−706.

(11) Wuensch, T.; Schulz, S.; Ullrich, S.; Lill, N.; Stelzl, T.; Rubio-Aliaga, I.; Loh, G.; Chamaillard, M.; Haller, D.; Daniel, H. The peptide transporter PEPT1 is expressed in distal colon in rodents and humans and contributes to water absorption. *Am. J. Physiol.: Gastrointest. Liver Physiol.* **2013**, *305*, G66−G73.

(12) Jappar, D.; Wu, S. P.; Hu, Y.; Smith, D. E. Significance and regional dependency of peptide transporter (PEPT) 1 in the intestinal permeability of glycylsarcosine: in situ single-pass perfusion studies in wild-type and *Pept1* knockout mice. *Drug Metab. Dispos.* **2010**, *38*, 1740−1746.

(13) Sanchez-Pico, A.; Peris-Ribera, J. E.; Toledano, C.; Torres-Molina, F.; Casabo, V. G.; Martin-Villodre, A.; Pla-Delfina, J. M. Non-linear intestinal absorption kinetics of cefadroxil in the rat. *J. Pharm. Pharmacol.* **1989**, *41*, 179−185.

(14) Garrigues, T. M.; Martin, U.; Peris-Ribera, J. E.; Prescott, L. F. Dose-dependent absorption and elimination of cefadroxil in man. *Eur. J. Clin. Pharmacol.* **1991**, *41*, 179−183.

(15) Weller, S.; Blum, M. R.; Doucette, M.; Burnette, T.; Cederberg, D. M.; de Miranda, P.; Smiley, M. L. Pharmacokinetics of the acyclovir pro-drug valaciclovir after escalating single- and multiple-dose administration to normal volunteers. *Clin. Pharmacol. Ther.* **1993**, *54*, 595−605.

(16) Hu, Y.; Chen, X.; Smith, D. E. Species-dependent uptake of glycylsarcosine but not oseltamivir in *Pichia pastoris* expressing the rat, mouse, and human intestinal peptide transporter PEPT1. *Drug Metab. Dispos.* **2012**, *40*, 1328−1335.

(17) Cheung, C.; Gonzalez, F. J. Humanized mouse lines and their application for prediction of human drug metabolism and toxicological risk assessment. *J. Pharmacol. Exp. Ther.* **2008**, *327*, 288−299.

(18) Stanley, L. A.; Horsburgh, B. C.; Ross, J.; Scheer, N.; Wolf, C. R. Drug transporters: gatekeepers controlling access of xenobiotics to the cellular interior. *Drug Metab. Rev.* **2009**, *41*, 27−65.

(19) Jiang, X. L.; Gonzalez, F. J.; Yu, A. M. Drug-metabolizing enzyme, transporter, and nuclear receptor genetically modified mouse models. *Drug Metab. Rev.* **2011**, *43*, 27−40.

(20) Boverhof, D. R.; Chamberlain, M. P.; Elcombe, C. R.; Gonzalez, F. J.; Heflich, R. H.; Hernández, L. G.; Jacobs, A. C.; Jacobson-Kram, D.; Luijten, M.; Maggi, A.; Manjanatha, M. G.; Benthem, J.; Gollapudi, B. B. Transgenic animal models in toxicology: historical perspectives and future outlook. *Toxicol. Sci.* **2011**, *121*, 207−233.

(21) Scheer, N.; Wolf, C. R. Xenobiotic receptor humanized mice and their utility. *Drug Metab. Rev.* **2013**, *45*, 110−121.

(22) Van Keuren, M. L.; Gavrilina, G. B.; Filipiak, W. E.; Zeidler, M. G.; Saunders, T. L. Generating transgenic mice from bacterial artificial chromosomes: transgenesis efficiency, integration and expression outcomes. *Transgenic Res.* **2009**, *18*, 769−785.

(23) Hu, Y.; Smith, D. E.; Ma, K.; Jappar, D.; Thomas, W.; Hillgren, K. M. Targeted disruption of peptide transporter Pept1 gene in mice significantly reduces dipeptide absorption in intestine. *Mol. Pharmaceutics* **2008**, *5*, 1122−1130.

(24) Hu, Y.; Xie, Y.; Keep, R. F.; Smith, D. E. Divergent developmental expression and function of the proton-coupled oligopeptide transporters PepT2 and PhT1 in regional brain slices of mouse and rat. *J. Neurochem.* **2014**, *129*, 955−965.

(25) Kou, J. H.; Fleisher, D.; Amidon, G. L. Calculation of the aqueous diffusion layer resistance for absorption in a tube: application to intestinal membrane permeability determination. *Pharm. Res.* **1991**, *8*, 298−305.

(26) Komiya, I.; Park, J. Y.; Kamani, A.; Ho, N. F. H.; Higuchi, W. I. Quantitative mechanistic studies in simultaneous fluid flow and intestinal absorption using steroids as model solutes. *Int. J. Pharm.* **1980**, *4*, 249−262.

(27) Chandler, K. J.; Chandler, R. L.; Broeckelmann, E. M.; Hou, Y.; Southard-Smith, E. M.; Mortlock, D. P. Relevance of BAC transgene copy number in mice: transgene copy number variation across multiple transgenic lines and correlations with transgene integrity and expression. *Mamm. Genome* **2007**, *18*, 693−708.
(28) van de Steeg, E.; van der Kruijssen, C. M.; Wagenaar, E.; Burggraaff, J. E.; Mesman, E.; Kenworthy, K. E.; Schinkel, A. H. Methotrexate pharmacokinetics in transgenic mice with liver-specific expression of human organic anion-transporting polypeptide 1B1 (SLCO1B1). *Drug Metab. Dispos.* **2009**, *37*, 277−281.
(29) van de Steeg, E.; Stránecký, V.; Hartmannová, H.; Nosková, L.; Hřebíček, M.; Wagenaar, E.; van Esch, A.; de Waart, D. R.; Oude Elferink, R. P.; Kenworthy, K. E.; Sticová, E.; al-Edreesi, M.; Knisely, A. S.; Kmoch, S.; Jirsa, M.; Schinkel, A. H. Complete OATP1B1 and OATP1B3 deficiency causes human Rotor syndrome by interrupting conjugated bilirubin reuptake into the liver. *J. Clin. Invest.* **2012**, *122*, 519−528.
(30) van de Steeg, E.; van Esch, A.; Wagenaar, E.; Kenworthy, K. E.; Schinkel, A. H. Influence of human OATP1B1, OATP1B3, and OATP1A2 on the pharmacokinetics of methotrexate and paclitaxel in humanized transgenic mice. *Clin. Cancer Res.* **2013**, *19*, 821−832.
(31) Scheer, N.; Balimane, P.; Hayward, M. D.; Buechel, S.; Kauselmann, G.; Wolf, C. R. Generation and characterization of a novel multidrug resistance protein 2 humanized mouse line. *Drug Metab. Dispos.* **2012**, *40*, 2212−2218.
(32) Ford, D.; Howard, A.; Hirst, B. H. Expression of the peptide transporter hPepT1 in human colon: a potential route for colonic protein nitrogen and drug absorption. *Histochem. Cell Biol.* **2003**, *119*, 37−43.
(33) Ogihara, H.; Saito, H.; Shin, B. C.; Terado, T.; Takenoshita, S.; Nagamachi, Y.; Inui, K.; Takata, K. Immuno-localization of H +/peptide cotransporter in rat digestive tract. *Biochem. Biophys. Res. Commun.* **1996**, *220*, 848−852.
(34) Groneberg, D. A.; Doring, F.; Eynott, P. R.; Fischer, A.; Daniel, H. Intestinal peptide transport: ex vivo uptake studies and localization of peptide carrier PEPT1. *Am. J. Physiol.: Gastrointest. Liver Physiol.* **2001**, *281*, G697−G704.
(35) Merlin, D.; Si-Tahar, M.; Sitaraman, S. V.; Eastburn, K.; Williams, I.; Liu, X.; Hediger, M. A.; Madara, J. L. Colonic epithelial hPepT1 expression occurs in inflammatory bowel disease: transport of bacterial peptides influences expression of MHC class 1 molecules. *Gastroenterology* **2001**, *120*, 1666−1679.
(36) Posada, M. M.; Smith, D. E. Relevance of PepT1 in the intestinal permeability and oral absorption of cefadroxil. *Pharm. Res.* **2013**, *30*, 1017−1025.
(37) Yang, B.; Smith, D. E. Significance of peptide transporter 1 in the intestinal permeability of valacyclovir in wild-type and PepT1 knockout mice. *Drug Metab. Dispos.* **2013**, *41*, 608−614.
(38) Dalmasso, G.; Nguyen, H. T.; Ingersoll, S. A.; Ayyadurai, S.; Laroui, H.; Charania, M. A.; Yan, Y.; Sitaraman, S. V.; Merlin, D. The PepT1-NOD2 signaling pathway aggravates induced colitis in mice. *Gastroenterology* **2011**, *141*, 1334−1345.
(39) Jappar, D.; Hu, Y.; Smith, D. E. Effect of dose escalation on the in vivo oral absorption and disposition of glycylsarcosine in wild-type and *Pept1* knockout mice. *Drug Metab. Dispos.* **2011**, *39*, 2250−2257.